(Preprint) AAS 17-267

TARGETING CISLUNAR NEAR RECTILINEAR HALO ORBITS FOR HUMAN SPACE EXPLORATION

Jacob Williams*, David E. Lee †, Ryan J. Whitley ‡,
Kevin A. Bokelmann §, Diane C. Davis ¶, and Christopher F. Berry †

Part of the challenge of charting a human exploration space architecture is finding locations to stage missions to multiple destinations. To that end, a specific subset of Earth-Moon halo orbits, known as Near Rectilinear Halo Orbits (NRHOs) are evaluated. In this paper, a systematic process for generating full ephemeris based ballistic NRHOs is outlined, different size NRHOs are examined for their favorability to avoid eclipses, the performance requirements for missions to and from NRHOs are calculated, and disposal options are evaluated. Combined, these studies confirm the feasibility of cislunar NRHOs to enable human exploration in the cislunar proving ground.

INTRODUCTION

In order to conduct sustained human exploration beyond Low Earth Orbit (LEO), spacecraft systems are being designed for a series of missions of increasing complexity. Regardless of the destination (the Moon, Mars, asteroids or beyond) there is a substantial set of common objectives that must be met. Part of the challenge of charting a space architecture for human exploration is finding suitable orbits to stage missions to multiple destinations. To that end, previous studies have indicated that cislunar orbits, and in particular Earth-Moon libration point orbits, are favorable for multi-mission staging.[1–3] Desirable properties of a staging orbit in the vicinity of the Moon include:

- Relatively easy access from the Earth to the destination orbit and back. Timely access is also important for crewed missions.
- Relatively easy access to Low Lunar Orbit (LLO) and the lunar surface, and back.
- Visibility of regions of the lunar surface not visible from Earth, to support human and/or telerobotic expeditions.
- Relatively easy departure to and arrival from deep space destinations beyond cislunar space. This is a focus not only for human missions to deep space destinations, but also for robotic missions returning large samples to a human-accessible orbit for scientific study.
- Relatively low propulsive requirements to maintain the orbit.

One category of libration point orbits of particular interest are the halo orbit families.[4] The current investigation focuses on a specific subset of the halo families known as Near Rectilinear Halo Orbits

*Aerospace Engineer, ERC Inc. (JSC Engineering, Science, and Technology Contract), Houston, TX, 77058
†Aerospace Engineer, Flight Mechanics and Trajectory Design Branch, NASA JSC, Houston, TX, 77058
‡Aerospace Engineer, Exploration Mission Planning Office, NASA JSC, Houston, TX, 77058
§Ph.D. Student, Aerospace Engineering and Engineering Mechanics, University of Texas, Austin, TX 78712
¶Aerospace Engineer, a.i. solutions, Inc., Houston, TX, 77058

(NRHOs).[5–7] Previous studies have demonstrated the favorability of NRHOs in a general sense against the criteria listed above.[3] The current study focuses on NRHOs in terms of techniques for generating trajectories, mission design and performance for crewed missions, and considerations for disposal trajectories.

In the Earth-Moon system, L_1 and L_2 NRHOs are characterized by close passage over one of the lunar poles. Both North and South NRHO families exist. The northern NRHOs reach their furthest distance from the Moon over the lunar North Pole, and the southern NRHOs achieve apolune over the lunar South Pole. Perfectly periodic in the Circular Restricted Three Body Problem (CR3BP) model*, NRHOs can be classified by their minimum periapsis radius (r_p) values with respect to the Moon (i.e., the radius of closest approach). NRHOs also exist in higher-fidelity force models as quasi-periodic orbits. The focus of the current study are NRHOs with $r_p < 6000$ km and orbital periods of about 8 days or less. The relationship between r_p and orbital period for the L_1 and L_2 halo families is shown in Figure 1.

GENERATING NEAR-RECTILINEAR HALO ORBITS

Solutions in the Circular Restricted Three Body Problem

One starting point for targeting an NRHO in the ephemeris model is to first generate a periodic NRHO in the CR3BP model. In the Moon-centered Earth-Moon rotating frame†, the x and z components of the rotating velocity, v_x and v_z, are equal to zero at $r_y = 0$ (when the orbit crosses the rotating $x-z$ plane at periapsis and apoapsis). In the current study, a multiple-shooting method is used to compute CR3BP NRHOs by specifying periapsis and apoapsis states with $r_y = v_x = v_z = 0$, propagating forward from periapsis and backward from apoapsis, and constraining full state continuity halfway between. The other state components (r_x, r_z, and v_y at both points) are control variables, as is the orbit period. Finally, r_p is also constrained to the desired value. Starting from a single converged solution with r_p at the lunar surface (about 1700 km), a continuation method is then used to generate solutions throughout the entire NRHO family. This process is repeated

*In the idealized CR3BP model, the Earth and Moon move in circular orbits about their barycenter, and the mass of the third body (the spacecraft) is negligible.

†The Earth-Moon rotating frame is useful when discussing halo orbits in the Earth-Moon system. The x-axis of this frame is defined to be along the instantaneous Earth-Moon position vector, the z-axis is along the instantaneous angular momentum vector of the Moon's orbit around the Earth, and the y-axis completes the orthogonal system. For these studies, the frame center will typically be the Moon, although it could be defined at the Earth, the barycenter or anywhere else in the system (such as a libration point). The frame can be used in the CR3BP or the ephemeris model. Rotating frames for other body pairs can also be defined.

Table 1: CR3BP Patch Points for the $r_p = 4500$ km South family case (the orbit period is 6.993 days). The states are given in the Moon-centered Earth-Moon rotating frame.

	Periapsis	1/8 Rev	1/4 Rev	3/8 Rev	1/2 Rev
r_x (km)	-247.122	6060.483	11467.119	14868.184	16023.074
r_y (km)	0.000000	19452.284	16269.487	8955.187	0.000
r_z (km)	4493.209	-34982.968	-56381.822	-68055.505	-71816.650
v_x (km/s)	0.000000	0.082677	0.059130	0.030451	0.000000
v_y (km/s)	1.444467	0.006820	-0.077120	-0.111682	-0.121971
v_z (km/s)	0.000000	-0.368434	-0.212112	-0.100368	0.000000

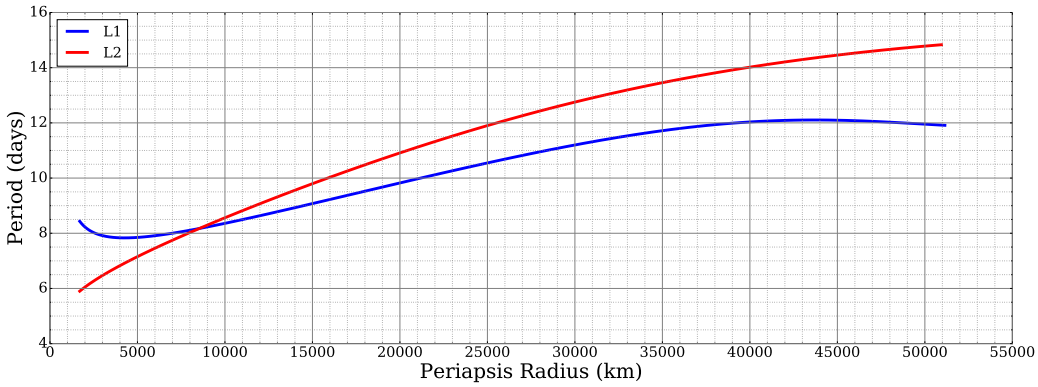

Figure 1: Orbit period versus periapsis radius for halo orbits in the Earth-Moon CR3BP model.

for both the L_1 and L_2 NRHO families to produce a database of orbits. The orbits are computed assuming an Earth-Moon distance of 384400 km, with the Earth and Moon gravitational parameters shown in Table 2. Patch points from this database of NRHOs, equally spaced in time, are then used to provide initial guesses for solutions in an ephemeris force model. Representative CR3BP patch points for an $r_p = 4500$ km NRHO (L_2, South family) are shown in Table 1. Note that the patch points are mirrored about the rotating frame $x - z$ plane, so the $[r_y, v_x, v_z]$ coordinates of the 3/4 rev patch point are simply the negative of the 1/4 rev ones. Also the North and South families are mirrored about the rotating frame $x - y$ plane, so the $[r_z, v_z]$ coordinates of one family are simply the negative of the other.

Solutions in the Ephemeris Model

There are various ways to generate NRHOs using some variation of a method that starts with patch points taken from a periodic CR3BP solution and uses multiple-shooting and targeting to produce a ballistic (or quasi-ballistic) trajectory in the ephemeris model.[9] In the literature a forward shooting method is frequently suggested (as shown in Figure 2a). An alternate method used in this study (shown in Figure 2b) applies both forward and backward shooting. The forward/backward shooting method is selected to help mitigate challenges presented by the close lunar approaches of the NRHO family of orbits. In this method, the trajectory segments are propagated forward and backward from the patch points and constrained in the center, avoiding forward-propagated segments constrained close to periapsis, where the state is changing rapidly. The forward/backward shooting method is found to exhibit better convergence properties with a smaller number of patch points. In the current investigation, patch points from periapsis (0-rev), apoapsis (1/2-rev) and halfway between on each side (1/4 and 3/4-rev), are taken from the CR3BP NRHO (as shown in Figure 2b). In the forward/backward method, a single rev contains 8 trajectory segments with 35 control variables and 24 equality constraints. If n_{revs} is the number of revs, then the total number

Table 2: Gravitational Parameters.[8]

Body	Gravitational Parameter ($\mathrm{km}^3/\mathrm{s}^2$)
Earth	398600.436233
Moon	4902.800076
Sun	132712440040.944

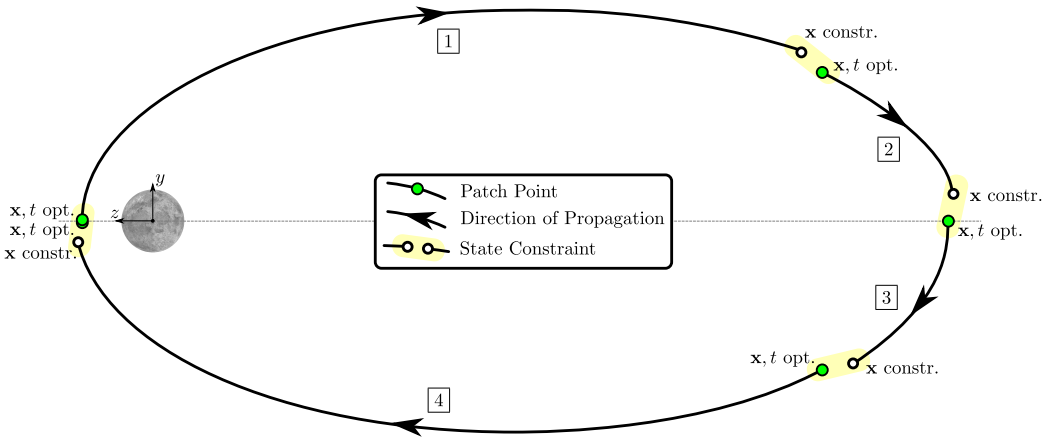

(a) Forward Shooting Method. In this method, the CR3BP NRHO patch points are propagated forward in time and constrained to match the state of the next patch point. The state and time of each patch point are control variables.

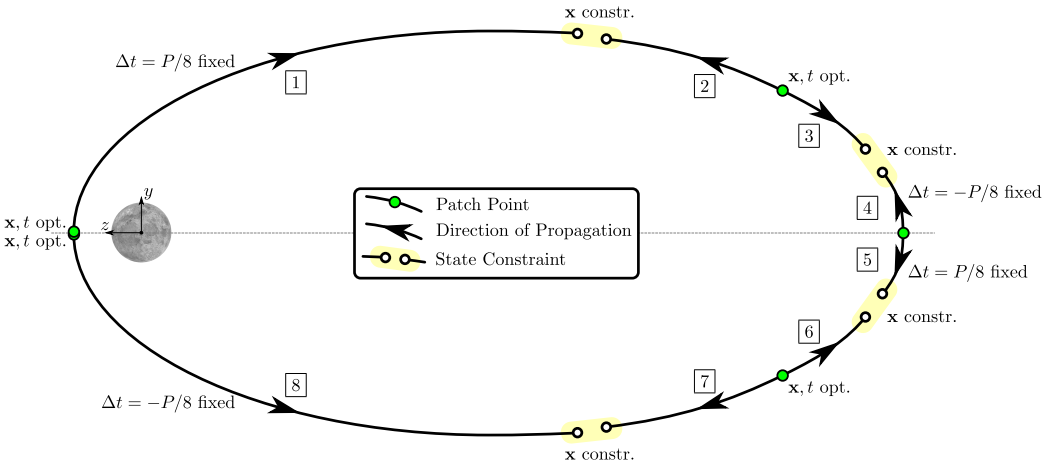

(b) Forward/Backward Shooting Method. The CR3BP NRHO patch points are propagated forward and backward and constrained near the middle. The state and time of each patch point are control variables. The fixed intermediate Δt values are taken from the CR3BP period (P), and the other Δt values are floating since the actual patch point epochs are adjusted during the targeting process.

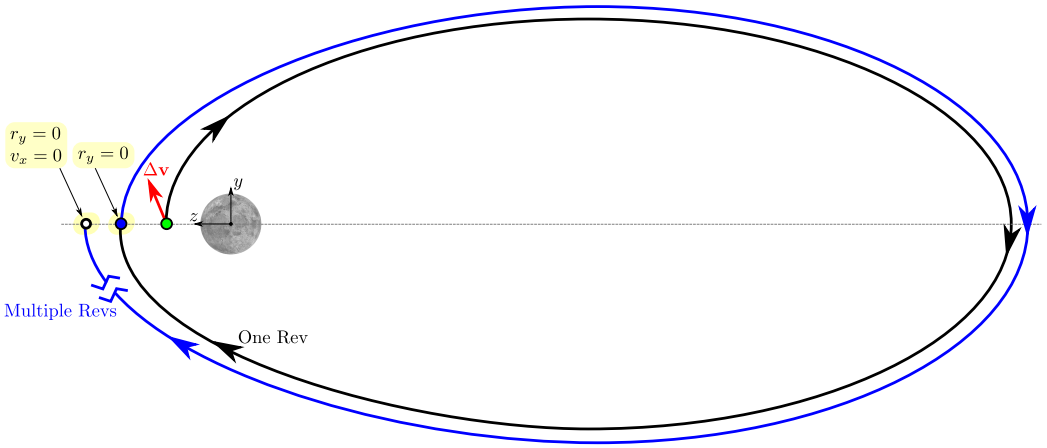

(c) Receding-Horizon Method. A Δv maneuver at periapsis targets an x-z plane crossing multiple revolutions later. The process is repeated at each periapsis passage.

Figure 2: NRHO Solution Methods (y-z Plane).

of control variables for the complete problem is $n = 28n_{revs} + 7$ and the total number of equality constraints is $m = 24n_{revs}$. Note that these are the same for the forward-only method.

The sequence of patch points can be repeated for as many revolutions of the orbit as desired to provide an initial guess for a long-duration ballistic orbit. For a 60-rev, $r_p = 4500$ km case (about 420 days), there are 1687 control variables and 1440 constraints (or 2,429,280 elements of the full Jacobian matrix). However, the Jacobian is very sparse, so the problem is suited to a sparse solver such as SNOPT.[10] A basic minimum-norm differential corrector solver can also be used, although it can be less efficient for very large problems. In the current study, the solution process is implemented in NASA's Copernicus spacecraft trajectory optimization program.[11] The force model includes the Moon, Earth and Sun, whose motions are modeled using the DE421 ephemeris.[8] The Moon's gravity is modeled using the GRAIL (GRGM660PRIM)[12] spherical harmonic model (truncated to degree and order 8). The Earth and Sun are modeled as point masses (using the gravitational parameters shown in Table 2). The trajectory segments are explicitly integrated using a variable-step size Adams method (DDEABM).[13] All gradients are computed numerically using finite differences (variational gradients[14] could also be used in this application, although it turned out not to be necessary). The SNOPT algorithm is used in "Feasible" mode (i.e., no objective function is specified) to achieve the midpoint position and velocity constraints, which can normally be done to within machine precision.

As a result, a ballistic trajectory is produced (with very small discontinuities at the midpoint constraint points). The iterative process is demonstrated to work for up to at least 100 revs, and typically convergence is achieved in fewer than 10 iterations. The method can be applied to the L_1 and L_2 NRHOs, and both the North and South families as shown in Figure 3a. The initial epoch of the first patch point is specified and can be held fixed or allowed to vary as part of the targeting problem.

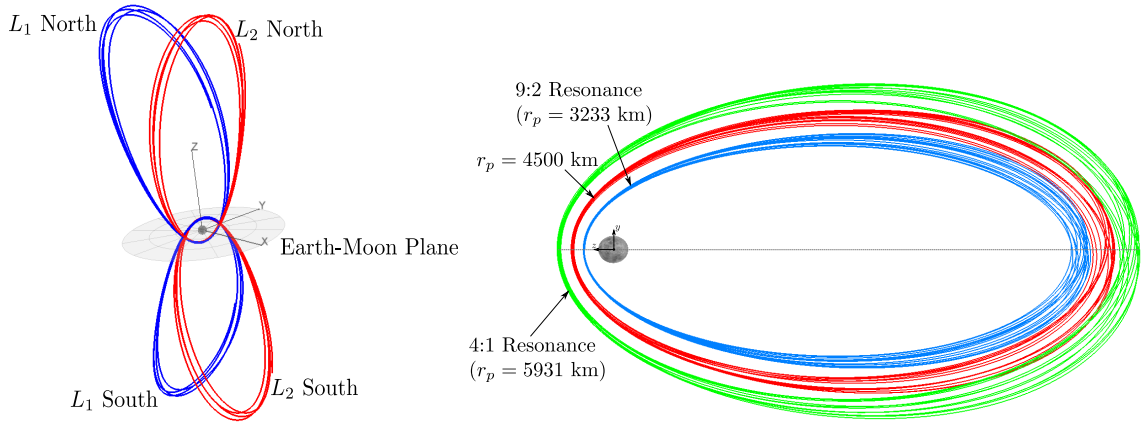

(a) Four Earth-Moon NRHOs with CR3BP $r_p = 4500$ km.

(b) Three NRHOs (L_2, South family) used in this study, shown for about 100 days (r_p values are from the CR3BP model).

Figure 3: Various Earth-Moon NRHOs shown in the Moon-centered Earth-Moon rotating frame. The orbits are targeted in an ephemeris model using the CR3BP patch points as an initial guess.

An example 20-revolution result for the $r_p = 4500$ km case is shown in Figure 4. To test the validity of the solution, the initial state is used to propagate the trajectory in a single integration, which produces a bounded NRHO for about 110 days. NRHOs are sensitive to perturbations, and

small discontinuities adding up over time cause an integrated NRHO to eventually depart from the reference. For NRHOs in the 4500 km range, this period is on the order of 100 days (the time to depart varies depending on the NRHO size and on integration and targeting tolerances.) However, in an operational environment, a spacecraft in an NRHO must perform periodic orbit maintenance maneuvers more frequently to stay in orbit long-term.[15]

Epoch	Nov 8, 2025 23:22:07.10353 TDB
r_x (km)	-1.259522004870315e+2
r_y (km)	1.209609406690672e+2
r_z (km)	4.357680596646485e+3
v_x (km/s)	-4.229621580376978e-2
v_y (km/s)	1.468560523456590e+0
v_z (km/s)	-3.538768970252955e-3

Figure 4: Example NRHO in the Ephemeris Model (L_2, $r_p = 4500$ km, South Family). Solved using the forward/backward shooting process, this orbit is stable for about 110 days.

An NRHO trajectory generated using these methods can also be used to initialize an alternate NRHO generation algorithm that uses a receding horizon approach,[16] as shown in Figure 2c. The receding horizon approach takes advantage of the knowledge that the rotating x-component of velocity, v_x, is equal to zero at the $r_y = 0$ plane crossing for a periodic halo orbit in the CR3BP. The initial state from an NRHO converged for several revolutions in the higher-fidelity force model is selected as an input for the algorithm. The initial state is propagated to periapsis, where a differential corrector targets a maneuver to achieve $v_x = 0$ at the $r_y = 0$ plane crossing some number n_{rev} of revolutions downstream (i.e. the "horizon"). The spacecraft is then propagated to the next periapsis, and the process is repeated.

The length of the horizon is selected based on the specific halo orbit and the allowed maneuver size. A longer horizon tends to yield significantly smaller Δv maneuvers, but also requires longer computation time. In addition, for NRHOs with very small or very large periapsis radii, a longer horizon can lead to difficulties with targeter convergence, since it is necessary to propagate a state for the full duration of the horizon without escaping from the NRHO or impacting the Moon. However, for L_2 NRHOs with periapsis radii ranging from about 2400 km to over 6500 km, a 10-revolution horizon effectively yields velocity discontinuities at periapsis with magnitudes of 1 mm/s or less when starting from a well-converged initial state.

The receding-horizon NRHO generation process can be continued indefinitely, creating a trajectory many years long. For example, an Earth-Moon L_2 South NRHO in 4:1 resonance with the lunar synodic cycle is associated with an $r_p \approx 5930$ km (see Figure 3b). The receding-horizon technique is applied with a 10-revolution horizon to create a 500-revolution (10-year) NRHO trajectory in a high-fidelity force model. Over the 10-year propagation, no individual targeting maneuver is larger than 0.52 mm/s, and the cumulative Δv totals 104 mm/s for 500 revolutions. Similarly, for a 9:2 lunar synodic resonant NRHO ($r_p \approx 3230$ km), the total cumulative Δv for a 500-revolution (9-year) propagation is 254 mm/s with a maximum individual targeting maneuver of 1.66 mm/s. These trajectories are effectively continuous; the velocity discontinuities at periapsis are small relative to noise and errors involved in the stationkeeping process, and they can effectively act as reference orbits for orbit maintenance. However, it is noted that larger discontinuities lead to larger stationkeeping costs; that is, maintaining a non-ballistic trajectory is, unsurprisingly, more expensive. If

stationkeeping to a reference orbit, it is important that the reference be effectively ballistically continuous in order to keep stationkeeping costs low. Details are given in a companion paper.[15]

Finally, another way to construct a long-duration reference is to use one of the above-mentioned patch point processes in a loop to construct a series of NRHOs that are patched together in time, but with either position and/or velocity discontinuities. This is done by fixing the initial epoch to match the final epoch of a previously-generated NRHO trajectory. The position or velocity can also be fixed (fixing position results in a Δv at the interface, fixing velocity results in a Δr, and fixing neither results in a full state discontinuity). This process can be repeated indefinitely, with each problem solved in sequence (in this way, it is similar to the receding horizon method). For an example $r_p = 4500$ km case, a 20 year NRHO can be constructed by patching together a series of 30-rev NRHO trajectories at apoapsis (fixing the position vector). The resultant trajectory is continuous in time and phase, and includes a Δv maneuver at apoapsis every 30 revs. The average magnitude of these maneuvers is about 13 m/s (patching at periapsis produces an average maneuver magnitude of about 74 m/s). Note that the magnitudes of these maneuvers are not being minimized, and this process is not meant to produce a flyable trajectory, but is used to create pseudo-continuous long-duration trajectories for various design studies, including the eclipsing studies described in the next section.

ECLIPSES IN NRHOs

A spacecraft in an NRHO can be subject to eclipses by the shadows of both the Earth and the Moon. It is important to understand the eclipse situation in the NRHO for two reasons: power generation and the thermal environment. First, most spacecraft in the NRHO will probably rely on solar power, so eclipses are likely to cause operational disruptions at least, and extended eclipse conditions could impose severe requirements on the power systems. But perhaps more importantly, the thermal environment during an eclipse in an NRHO can be extremely cold – the spacecraft can be far from the thermally emitting gravitational bodies, and then shielded from solar thermal emissions as well. It may be difficult to design hardware to survive extended periods in such an extreme thermal environment.

The Eclipse Environment for a Representative NRHO

The first order of business was to understand the frequency, duration, and depth of eclipses for a typical NRHO in our range of interest. For this purpose, an L_2 South NRHO with an r_p of 4500 km was selected, with a period of roughly seven days. Eight trajectory cases were then generated, each of roughly 19 years duration in order to cover the full 18.6 year lunar nodal cycle, with each successive case offset in initial periapsis epoch (and hence phase) by one day. These trajectories were generated using the pseudo-continuous method previously described.

For the 4500 km L_2 South NRHO cases, eclipses by the Earth occurred about once a year on average, but somewhat sporadically and sometimes with multi-year gaps between occurrences (see Figure 5). Over half of the eclipses by the Earth included a period of totality. Overall durations of up to 4.83 hours were observed, with periods of total eclipse of up to 2.57 hours.

Eclipses by the Moon were much more frequent, averaging around seven events per year (see Figure 5). Of those, around 95 percent included a period of totality. Eclipses by the Moon were much shorter on average than those by the Earth. Overall durations of up to 1.48 hours were observed, with periods of total eclipse of up to 1.42 hours. See Figure 6 for histograms of eclipse duration.

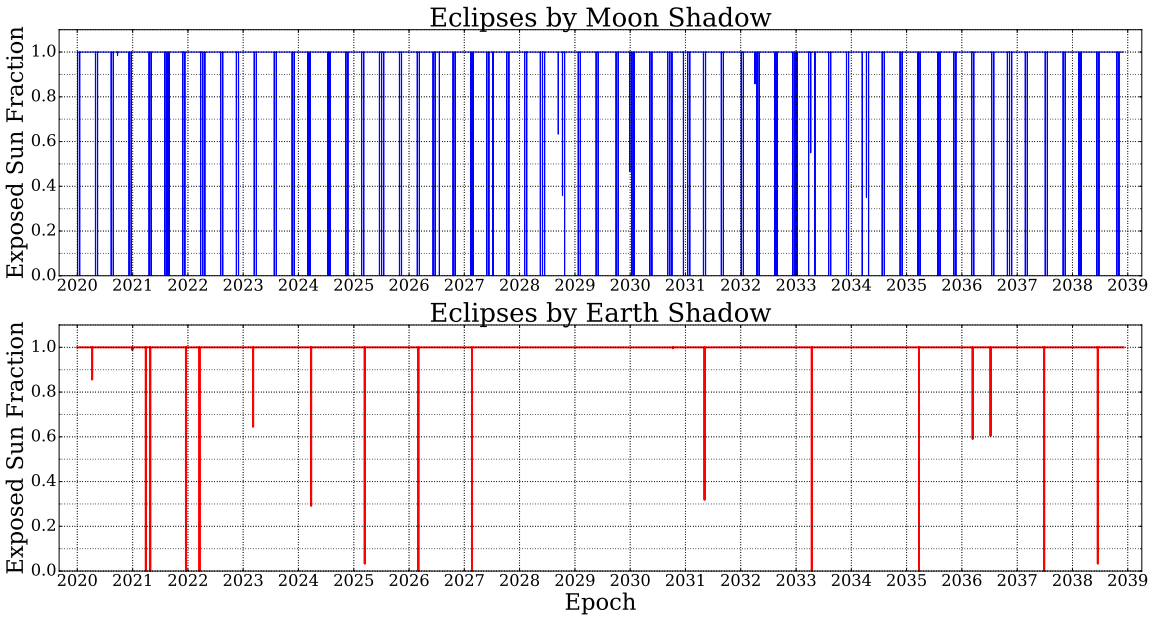

Figure 5: Typical Eclipse History for NRHOs with r_p=4500 km.

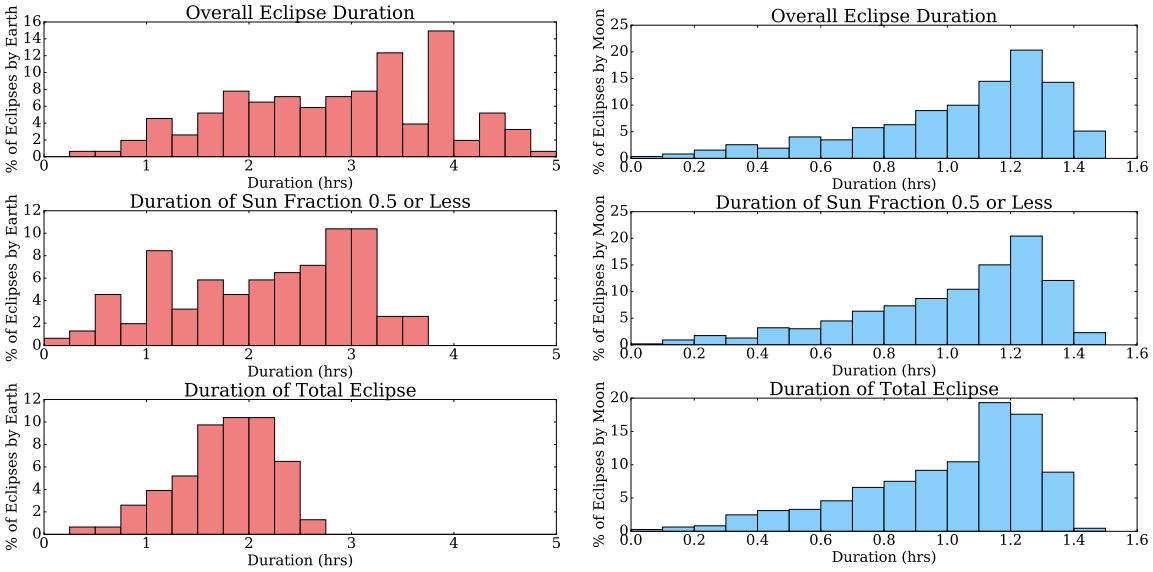

(a) Eclipses by the Earth.

(b) Eclipses by the Moon.

Figure 6: Histograms of duration at or below various levels of exposed sun fraction for eclipses by the Earth and Moon for NRHOs with r_p=4500 km.

It is believed that eclipses by the Earth might be avoided or minimized with advanced planning and strategic maneuvers of relatively modest magnitude. This is because the NRHO trajectory is relatively far from the Earth, and sweeping around the Earth at roughly lunar distance, and because the shadow of the Earth is relatively narrow compared with those distances. A small change in timing, a shift in periapsis radius (and hence phase rate) far enough in advance should be enough to allow the spacecraft to avoid a specific eclipse event.

Avoiding eclipses by the Moon would be significantly more difficult in general, however, because they occur when the spacecraft is in the part of the NRHO that is very close to the Moon. The shadow of the Moon covers too wide an angular range, in a region the spacecraft must pass through, to avoid most of these eclipses. However, since the duration of the eclipses by the Moon are much shorter, this may be a manageable problem.

Avoidance of Eclipses with Lunar Synodic Resonance

An NRHO with a period resonant with the average lunar synodic period* would give (roughly) repeating geometry in the Earth-Sun rotating frame. By selecting the initial phase, we might avoid some or all eclipse events. By comparing the orbit periods of NRHOs from the CR3BP model (see Figure 1) with different potential resonance periods, some promising resonance cases were identified (see Table 3). Two L_2 resonance cases were selected for further study: 4 NRHO revs per 1 lunar month (4:1), and 9 NRHO revs per 2 lunar months (9:2). These NRHOs are illustrated in Figure 3b. For both cases, we generated 19 year pseudo-continuous trajectory approximations (as described previously) in the ephemeris model, adjusting them for proper initial phase and phase rate by a rather intensive trial and error process using the graphics capabilities of Copernicus.

Figure 7 illustrates the repeating geometry of the 4:1 lunar synodic resonant NRHO in the Sun-Earth and Sun-Moon rotating frames. In each of these frames the central axis of the respective eclipse cone lies along the line from the Sun to the eclipsing body as it projects out the far side of the eclipsing body. The 4:1 lunar synodic resonant NRHO offers broad margins between the spacecraft and the eclipse cones of both the Earth and the Moon, and was able to completely avoid eclipses over the entire period.

*The lunar synodic period, about 29.53 days on average, is the time required for the Moon to complete a revolution about the Earth with respect to the line between the Earth and the Sun. This is commonly referred to as a lunar month.[17]

Table 3: NRHO Periapsis Radii Corresponding to Selected Lunar Synodic Resonance Ratios (cases of interest in bold). Based on CR3BP model. Note that the r_p values for cases converged in the ephemeris model will vary somewhat.

Lunar Synodic Periods	NRHO Revs	NRHO Revs per Lunar Synodic Period	NRHO Period (days)	NRO Periapsis Radius for L_1 NRHOs (km)	NRO Periapsis Radius for L_2 NRHOs (km)
1	3	3	9.8435	20130	15200
1	4	4	7.3826	–	**5750**
2	7	3.5	8.4373	10576	9525
2	9	4.5	6.5624	–	**3249**

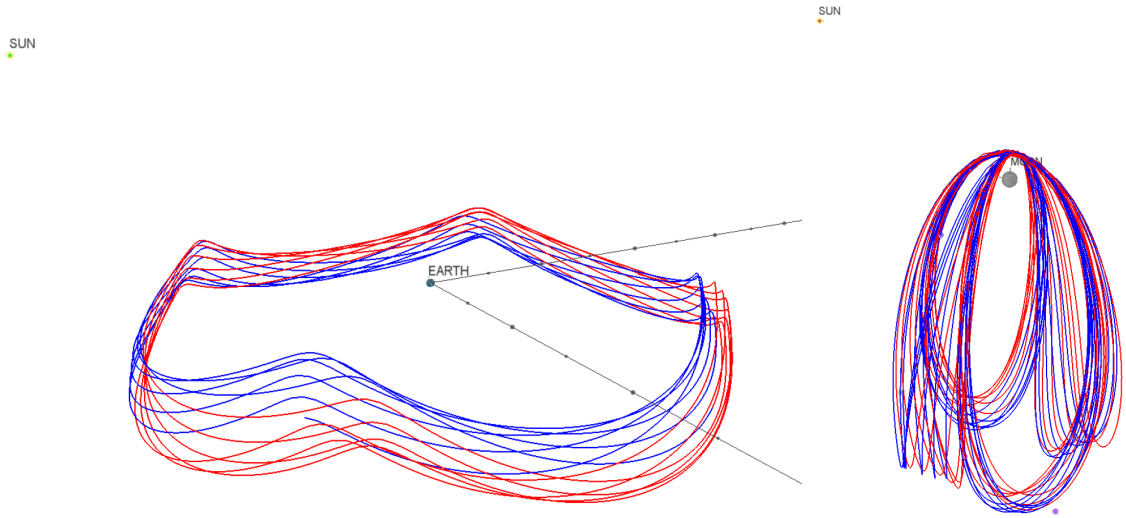

(a) Earth-centered Sun-Earth rotating frame

(b) Moon-centered Sun-Moon rotating frame

Figure 7: 4:1 lunar synodic resonant NRHO in Sun-eclipsor rotating frames to illustrate repeating geometry.

Figure 8 illustrates the repeating geometry of the 9:2 lunar synodic resonant NRHO in the Sun-Earth rotating frame. In the one year of the trajectory illustrated, the trajectory avoids the Earth shadow axis. The margins, however, are much smaller than in the 4:1 resonance case. Figure 9 shows the history of eclipses by both the Earth and Moon for 19 years in the 9:2 lunar synodic resonant NRHO. The 9:2 trajectory case shown was able to avoid eclipses by the Earth for over 12 years. Eclipses by the Moon, however, were frequent, averaging about 10.5 events per year. These were found to be relatively short in duration with a maximum overall duration of under 1.3 hours and a maximum duration of totality under 1.2 hours.

It is suspected that with refinement of the pseudo-continuous model for the 9:2 resonance trajectory, a case with no eclipses by the Earth over 19 years could be found. However, because NRHOs are quasi-stable, in reality a spacecraft operating in an NRHO will have to perform periodic corrections to maintain the orbit. Particularly in the case of the 9:2 resonant NRHO, the orbit maintenance scheme may need to include provisions for phase control. In general, this would involve some control or biasing of the periapsis radius, in order to manage the phasing rate to maintain or correct the phase of the trajectory in the Sun-Earth frame. The 4:1 resonant NRHO might require this as well, but probably to a lesser degree as the margins are much broader.

TRAJECTORY DESIGN AND PERFORMANCE FOR MISSIONS TO NRHOs

Our mission design effort was focused on developing mission designs and understanding performance characteristics for missions delivering a human crew from the Earth to an NRHO and then bringing them back. The early mission studies made the assumption that the spacecraft could insert into the NRHO at any point and any epoch. There was no requirement to match position or phase with a spacecraft already in the NRHO. We called this the “free-phase” condition. These studies

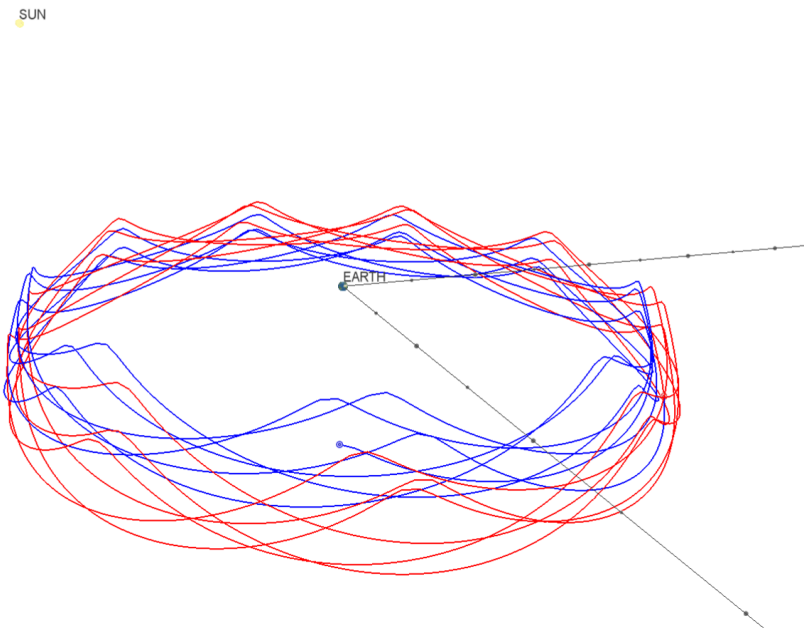

Figure 8: 9:2 lunar synodic resonant NRHO in Earth-centered Sun-Earth rotating frame to illustrate repeating geometry.

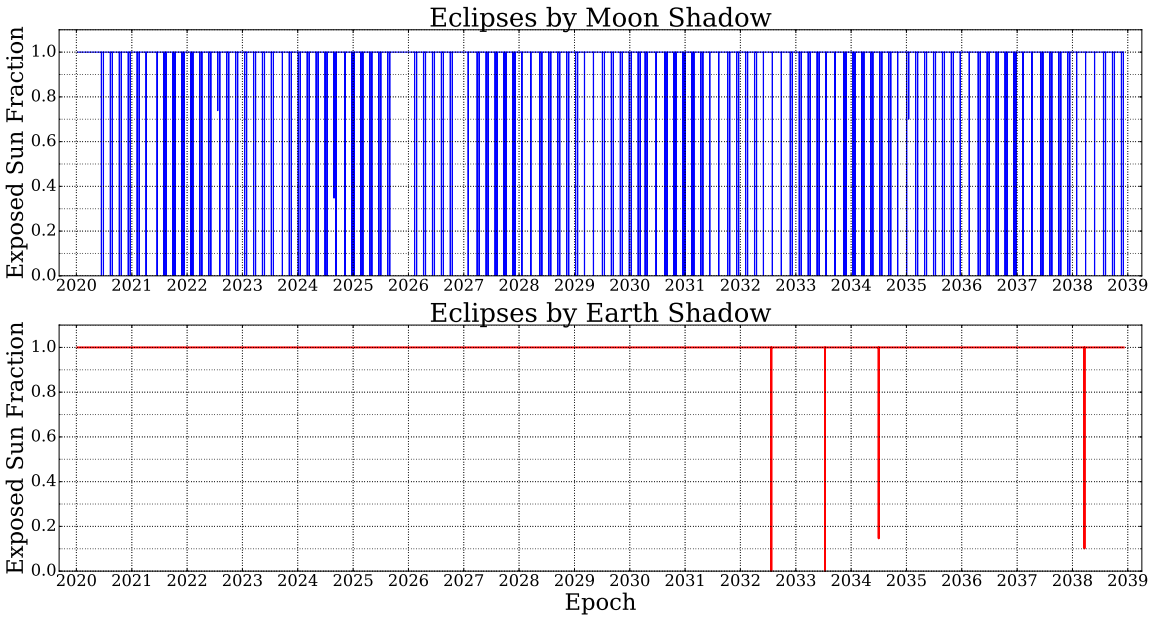

Figure 9: Eclipse History for 9:2 Lunar Synodic Resonant NRHO over 19 years.

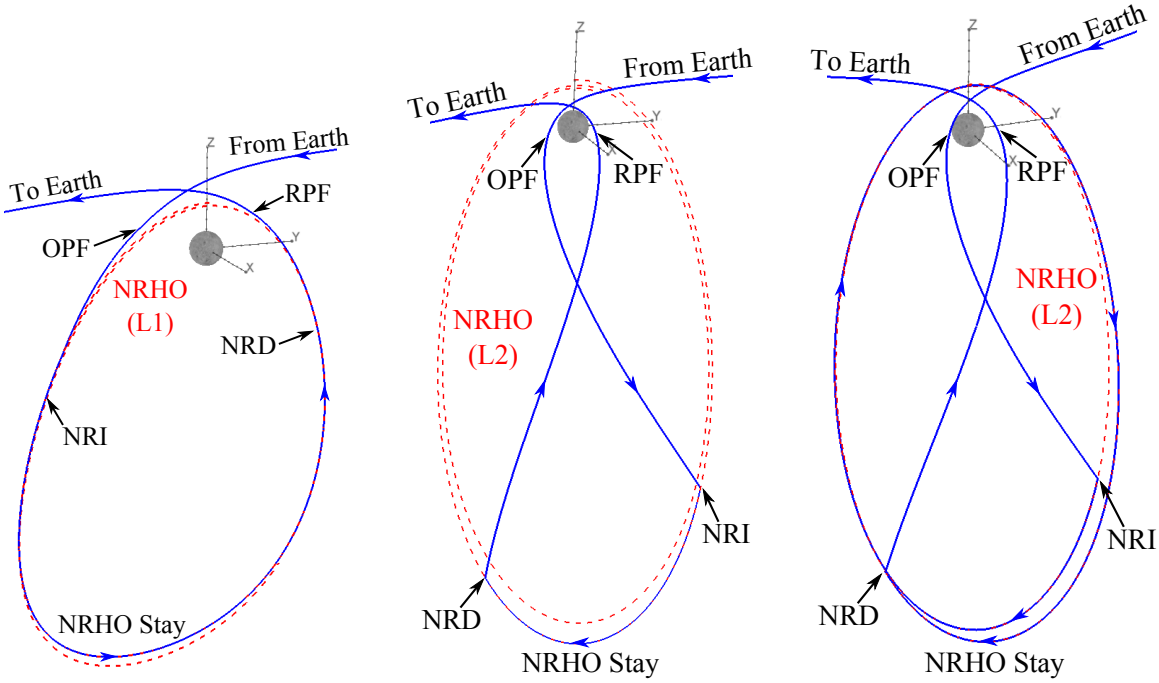

(a) L_1 Single Rev (7 days). (b) L_2 Short Stay (3-4 days). (c) L_2 Long Stay (9.5-11 days).

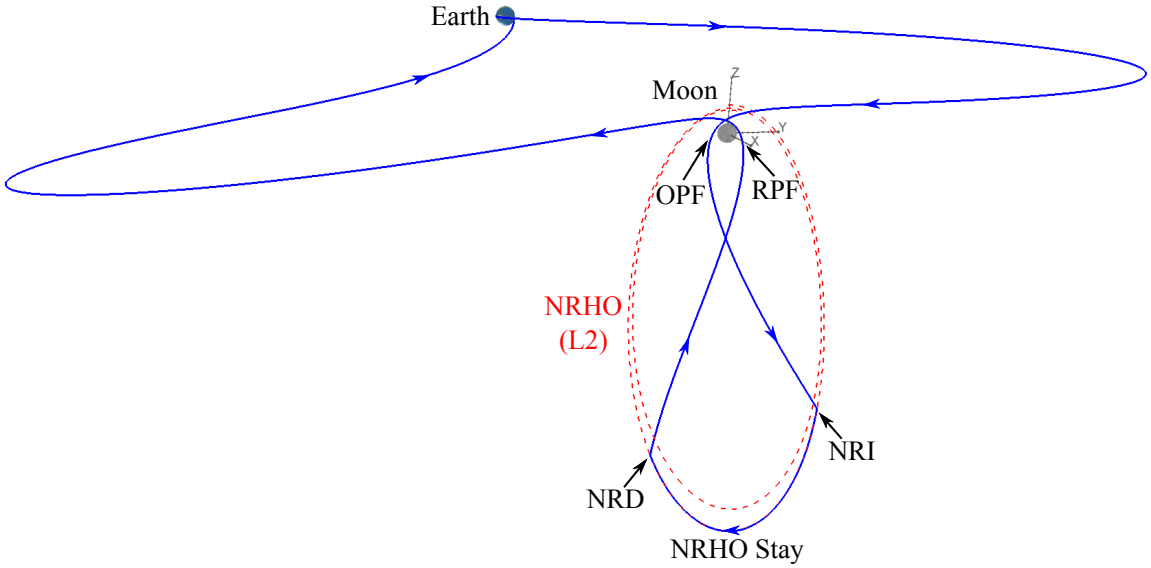

(d) Full Trajectory for L_2 Short Stay.

Figure 10: Roundtrip Missions to Earth-Moon NRHOs ($r_p = 4500$ km, South Families) Shown in the Earth-Moon Rotating Frame. For each mission type, Orion must perform four major translational maneuvers (OPF, NRI, NRD, and RPF). The L_2 cases include both "short stay" and "long stay" mission types. Stay times in the NRHO are shown in parentheses.

were realistic for missions delivering first elements (in some cases at least) or stand-alone payloads, and they gave us a general idea of the performance space.

However, once an initial element had been delivered to the NRHO, subsequent missions would have to rendezvous with the components already in place. This would require arrival in the NRHO at an appropriate combination of phase and epoch to place the arriving vehicle in the same general region of the orbit as the spacecraft already there. (This is also true for cases where we wish to control the phase of the NRHO for eclipse management purposes, in this case even for the initial missions.) We refer to this as the "fixed-phase" or rendezvous condition, and our final mission design studies looked at these rendezvous mission opportunities and how the performance for those missions compared with the free-phase studies.

Ground Rules and Assumptions for Mission Design Studies

These mission design studies are based on a common set of ground rules and assumptions, with a few variations over time:

- The Orion spacecraft was used for the crewed mission to an NRHO. The initial mass of Orion at separation was assumed to be 27000 kg , including 8086.4 kg of propellant available for translational maneuvers. The Orion Main Engine (OME) has a thrust of 6000 lbf (26689.33 N) and an I_{sp} of 315.1 s. Orion also has 8 Auxiliary (Aux) thrusters with a total thrust of 3760 N, and an I_{sp} of 309.9 s. However, plume losses and off-pulsing for attitude control mean the effective thrust will be lower: We assumed 3512.98 N.
- Orion was assumed to be launched on the Space Launch System (SLS) booster. An Earth-fixed LEO insertion state was used to approximate a due-east SLS launch to a roughly 185×185 km LEO circular parking orbit.
- The duration in LEO prior to Trans-Lunar Injection (TLI) was restricted to between 0 and 105 minutes. We did not account for a failed TLI or second TLI opportunity scenario.
- The TLI maneuver was approximated by an impulsive maneuver constrained such that the post-TLI $C_3 \leq -1.5$ km^2/s^2 and TLI impulsive $\Delta v \leq 3159.767$ m/s. The Δv constraint is necessary because we are allowing an out-of-plane component of the TLI burn. 3159.767 m/s is roughly the Δv to achieve a C_3 of -1.5 km^2/s^2 from this parking orbit using a gravity turn.
- Orion delivers a 10 t payload to the NRHO.
- Orion returns to a target line at atmospheric Entry Interface (EI) consistent with a splashdown at a point off the coast of southern California, near San Clemente Island.[18]

The basic mission design methodology using NASA's Orion and SLS vehicles is based on earlier studies of crewed missions to Distant Retrograde Orbits (DROs),[18] which in turn were based on previous analyses of missions to halo orbits.[19] For the baseline missions to L_2 NRHOs (see Figure 10), Orion must perform four major deterministic translational maneuvers:

- The Outbound Powered Flyby (OPF) maneuver near the Moon.
- The NRHO Insertion (NRI) maneuver – The arrival maneuver to insert into the NRHO.
- The NRHO Departure (NRD) maneuver – The departure maneuver to leave the NRHO, targeting a lunar flyby.
- The Return Powered Flyby (RPF) maneuver near the Moon, which targets Earth EI.

These studies included solutions for both ascending and descending TLI geometry cases. A TLI maneuver is considered ascending if it is closer to the ascending node of the parking orbit, and descending if it is closer to the descending node. The early studies used some impulsive burn ap-

proximations, while later studies (particularly starting with the Aux Abort studies) switched almost entirely to finite burns, with the exception of the TLI which was modeled as impulsive in all cases.

Preliminary Mission Scenarios

We first assessed the feasibility of various destination NRHOs and mission scenarios. Missions to both L_1 and L_2 NRHOs were considered, both with an r_p of 4500 km. The L_2 missions had stay times in the NRHO optimized in the vicinity of 1.5 revs, amounting to 9.5-11 days. The L_1 missions had stay times just short of a full rev. (The period of the 4500 km L_1 NRHO was 7.83 days, versus 7 days for the L_2 NRHO.) In this initial set, we found that all of the mission scenarios we tested appeared to be feasible. Missions in all categories had launch opportunities almost daily. In general, missions to L_1 NRHOs required significantly less Orion propellant than missions to L_2 NRHOs. L_1 missions with single burn insertion and departure proved to be feasible. Also, L_2 extended missions (with unconstrained durations) required less Orion propellant than missions limited to 21 days total duration. Although the missions to the L_1 NRHOs required less propellant, missions to L_2 NRHOs were deemed to be more suitable for non-performance-related reasons – for instance, visibility to the lunar far side for potential communications and telerobotics support to surface missions.

We also conducted a 90 day study to compare missions to L_2 North versus L_2 South NRHOs. In this study, both North and South NRHOs had $r_p = 4500$ km, and the missions were limited to 21 days total duration, with the stay time in the NRHO optimized within a range between > 1 and < 2 revs. Missions to the L_2 South NRHOs required significantly less propellant than those to the L_2 North NRHOs. We determined that this was because all of our mission scenarios were returning to a splashdown in the northern hemisphere, making the problem inherently asymmetrical. The particular geometry of the lunar flybys on the return trip is what makes the difference - the missions to the L_2 South NRHOs with their northern flybys are more compatible with the southern approach to a northern splashdown back on Earth. (This is analogous to differences in performance between the ascending and descending TLI opportunities.)

For all of the mission studies using the free-phase assumption (i.e. no rendezvous), we employed a three step process to optimize round trip missions from Earth to the NRHO. First, an optimized "approximate" solution was converged using NRHO segments based on the uncorrected CR3BP patch point data to position the arrival and departure states. These segments were allowed to float in epoch to permit optimization of the overall trajectory problem. The epoch was then extracted from the approximate NRHO and used to generate an NRHO in the ephemeris model with phasing matching the approximate solution (using the process outlined earlier). The states from this real-ephemeris NRHO were then inserted into the overall trajectory model, with the epoch fixed (the insertion and departure were allowed to vary, but the NRHO phase was fixed). The overall trajectory was then reoptimized, resulting in an end-to-end optimized mission using a high-fidelity force model.

19 Year Performance Scan

We then carried out an extended study of mission performance, 19 years in duration, in order to understand how performance might vary over the 18.6 year lunar nodal cycle. These cases were again to an L_2 South NRHO with $r_p = 4500$ km. The total mission duration was again limited to 21 days, and the stay time in the NRHO was optimized within a range between > 1 and < 2 revs.

Again, feasible mission opportunities were found to be available on an almost daily basis (see

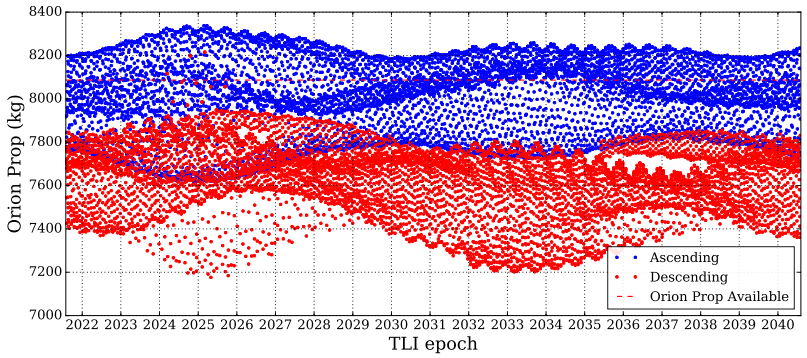

Figure 11: Total Orion Propellant from 19 Year Scan: Missions to L_2 South NRHOs with $r_p = 4500$ km, total mission duration < 21 days, NRHO stay time > 1 and < 2 revs. Includes delivery of a 10 t payload to the NRHO.

Figure 11). Also, opportunities with descending TLI maneuvers generally had lower Orion propellant usage than those with ascending TLIs (as we had seen in previous cases). The time span of the previous short studies turned out to be among the most challenging periods of the 19 year range.

Return Flyby Aux Aborts

An "Aux Abort" is a scenario where the OME fails to perform any of the four major translational maneuvers required for an Orion mission to an L_2 NRHO. In this case, the immediate priority shifts to returning the crew to Earth as quickly and safely as possible. At this point, the Orion Aux thrusters are employed to initiate a maneuver or sequence of maneuvers to bring the crew home. The particular maneuver sequence depends on which maneuver execution fails.[18]

We first looked at the Aux Abort at the RPF maneuver. This is the powered flyby maneuver that sends the Orion spacecraft back towards the Earth. The Aux Abort for this maneuver is essentially a longer version of the nominal maneuver - a single burn powered flyby. It is, however, significantly longer, as the Aux propulsion system has around 14% of the thrust of the OME (and even less when off-pulsing for attitude control is considered).

We quickly found that Aux Abort at the RPF maneuver was not feasible for most opportunities, unless it was included in the initial mission optimization. This is perhaps not surprising in retrospect, considering the lower thrust levels, and that there is bound to be at least a brief delay as the system switches over to the Aux system and the spacecraft slews to the new burn attitude. The timing of this maneuver is also very critical, as the spacecraft is moving very rapidly during its close flyby of the Moon – a short delay can result in the burn being in a badly suboptimal location.

The implication was that we would need to include the Aux Abort maneuver for RPF in our initial mission optimization, in order for it to be reliably available. This was not without cost, since we would be modifying the mission profile and the nominal RPF maneuver in particular. (The nominal RPF maneuver would be shifted slightly earlier.) There would be a performance impact, but feasible mission opportunities were still available for most launch days in the study period. Our later studies would, in fact, include the RPF Aux Abort contingency as part of the initial mission optimization.

Missions to Lunar Synodic Resonant NRHOs

As interest developed in lunar synodic resonant NRHOs due to properties for eclipse management, we began to assess missions to these orbits as well. We conducted two sets of 90 day studies for two different mission scenarios.

We initially studied missions limited to 21 days total duration, with stay times in the NRHO optimized within a range between > 1 and < 2 revs. The destination NRHOs had periapsis radii of 3200 km (approximating the 9:2 resonance case), 4500 km (for reference), and 5900 km (approximating the 4:1 resonance case). For these cases, we found that the 5900 km 4:1 case had some limitations to opportunities due to high Orion prop usage, while the others had feasible opportunities on a daily or near daily basis (see Figure 12a).

We also became interested in "short stay" missions, where Orion would stay only 3-4 days in the NRHO (less than a full rev). This stay time was thought to be adequate for Orion to perform checkout and deployment operations for new elements on early missions, while reducing mission durations well below the 21 day limitation. Studies of the short stay missions showed that all three of the L_2 South NRHO geometries under consideration had daily mission opportunities with practically identical performance. The previous differences were apparently due to the 21 day mission duration constraint (see Figure 12b).

Performance for Rendezvous (Fixed-Phase) Mission Scenarios

The previous analyses were unconstrained in phase at arrival (free-phase condition, as discussed previously). We will now consider cases where we have to either rendezvous with a spacecraft already in the NRHO, or simply insert to match an NRHO of pre-determined phase for eclipse management purposes (i.e. the fixed-phase or rendezvous condition). The methodology for optimizing fixed-phase mission trajectories was slightly different from that for the free-phase missions. Since the spacecraft flies to the same NRHO with the same phase every time, we generated a continuous NRHO trajectory and exported it to a SPICE ephemeris kernel, which we used as the target orbit for all the trajectories for that set of r_p cases.

For our fixed-phase studies, we conducted 90 day scans for short-stay type missions. Stay time in the NRHO was constrained to be ≥ 3 days. These studies considered NRHOs with r_p values of

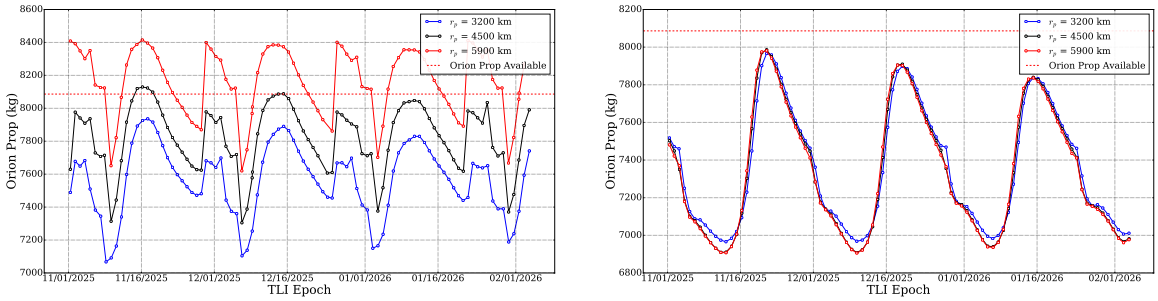

(a) 21 day missions with NRHO stay times of 9.5-11 days.

(b) Short stay missions with NRHO stay times of 3-4 days.

Figure 12: Performance comparison for missions to lunar synodic resonant NRHOs: 21 day limited missions versus short stay missions.

both 3233 and 5931 km. We also carried out a study where the 3233 km NRHO was phase shifted by 180° (i.e. the initial periapsis epoch was offset by half of the NRHO period).

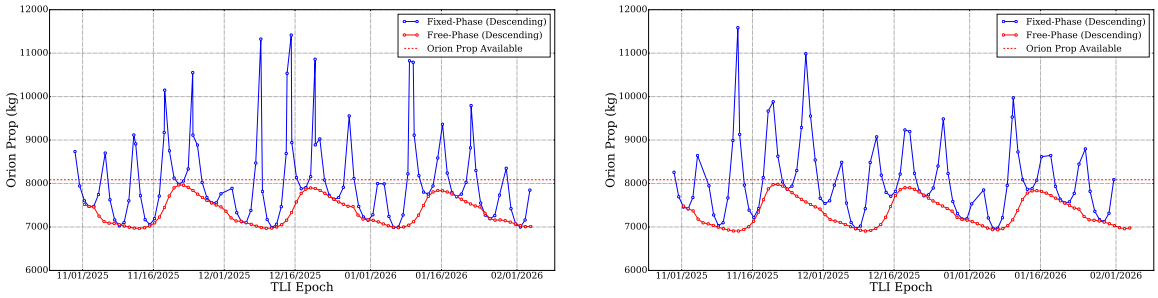

(a) $r_p = 3233$ km (4:1 lunar synodic resonant). (b) $r_p = 5931$ km (9:2 lunar synodic resonant).

Figure 13: Comparison of Orion Propellant for Fixed-Phase and Free-Phase: Short stay missions to lunar synodic resonant NRHOs.

We found that in order to minimize Orion propellent usage, the optimizer was adjusting the outbound trip times to keep the arrival in and departure from the NRHO near the favorable regions of the NRHO for those maneuvers. In terms of Orion propellant used, the rendezvous missions would approach the performance of the free-phase missions once per NRHO period. At these points near the phase match, there would typically be from 3 to 5 consecutive feasible rendezvous mission opportunities, with the best approaching the performance of the free-phase cases (see Figure 13). For the short stay missions examined, this means that there would be multiple sets of launch opportunities each month, with each set spanning 3 to 5 consecutive days. The results also indicate that, at least broadly, the previous free-phase results can be used to gain insight into the general performance situation for fixed-phase trajectories.

DISPOSAL FROM NRHOs

If the NRHO is to be used as a staging post, it will likely be necessary to dispose of spent stages, waste or even find favorable end-of-life conditions for portions of a potential long-term human orbital habitat. To that end, the sensitivity of the NRHO regime was quantified by applying various levels of Δv to target a diverse set of end conditions. In this analysis, the disposal was limited to a single small impulse to leave the habitat along a purely ballistic trajectory. The main controls were the time of departure and the direction of the impulse. Due to these limitations, there is interest in identifying what disposal options are possible. The primary goal was to simply identify what can be achieved within the restricted design space, and leave the detailed analysis for later work.

The disposal trajectories were investigated via a double grid search approach for a given constant impulse magnitude. Two relatively small impulse magnitudes are considered: 1 m/s and 5 m/s. The first grid variable is the location of the departure impulse along the NRHO, τ, measured as elapsed time from a reference periapsis. A variable step size in time is used to avoid grid points bunching at apoapsis and spreading at periapsis. The step size is simply a reference step scaled by the current orbit velocity in the rotating frame: $\Delta\tau = \Delta\tau_{ref}/v(\tau)$. At each impulse location a second search is run over the impulse direction. The direction consists of two angular variables, α and β, measuring the azimuth and polar angles of the impulse relative to the rotating velocity. The two variables are grouped together allowing for a single grid search that spans the sphere of possible directions.

Each resultant disposal trajectory is propagated for short and long term time scales. Short term is considered 30 days after impulse, providing insight into the immediate behavior of the departure. The long term is 120 days post-impulse, although longer time frames are considered for some point studies. The trajectory state at the end of both times is evaluated to categorize the departure behavior. Note that only the end states are considered, no analysis is done on the trajectory state prior to or after the end of propagation.

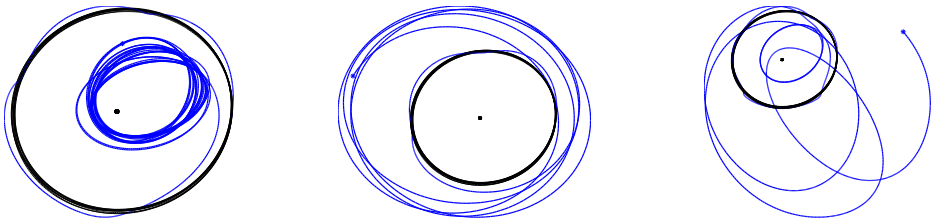

(a) Interior (b) Exterior (c) Crossing

Figure 14: Notional examples of the interior, exterior, and Moon-crossing disposal trajectories (inertial frame with the Moon's orbit and the Earth for reference).

A total of seven general trajectory types are identified: interior, exterior, Moon-crossing, near-Moon, Earth impact, Moon impact, and heliocentric escape. The first three trajectory types remain bound to the Earth-Moon system, characterized by the shape of the orbit with respect to the Moon's orbit. Interior trajectories remain within the Moon's orbit, exterior trajectories are beyond the Moon's orbit, and Moon-crossing has phases at both levels. Figure 14 shows examples of the three bound cases. The near-Moon category denotes departures that are within 1.5 times the Moon's sphere of influence at the time of evaluation. Impact trajectories intersect the surface of their respective body, while heliocentric escape occurs when the trajectory departs the Earth-Moon system. For the purposes of disposal, the impact and escape categories are of most practical interest as these trajectories are effectively "permanent" disposals that do not contribute to the accumulation of Earth-orbiting debris.

Figure 15a visualizes the "permanent" disposal possibilities for the 1 m/s impulse. Markers are added on the NRHO, indicating departure locations where there exists some impulse direction that results in the respective disposal category. All the disposal trajectories remain within the Moon's influence for at least 30 days and so only the 120 day results are shown. In the long term, every location has at least one impulse direction that leads to a heliocentric escape trajectory. In fact, heliocentric escapes are among the most common, accounting for nearly a third of all propagated disposals. This result enables significant freedom and redundancy if targeting a heliocentric escape: there is no window of opportunity that can be missed if there is an error or delay in the timing of the maneuver. For the Moon Impact case there is no such freedom of choice. The majority of the impulse locations are isolated or have only one adjacent point. There is a series of locations just after periapsis, equivalent to a relatively small departure window of approximately 1.3 hours. No Earth-impacting disposals are found within 120 days, although they do exist at longer propagation times.

Figure 15b shows the disposal visualization for a 5 m/s impulse. As expected, the larger maneuver enables faster departure from the Moon and disposals within 30 days are possible. In particular,

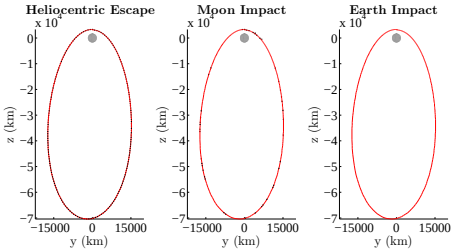

(a) 1 m/s Impulse Cases Within 120 day Time Frame.

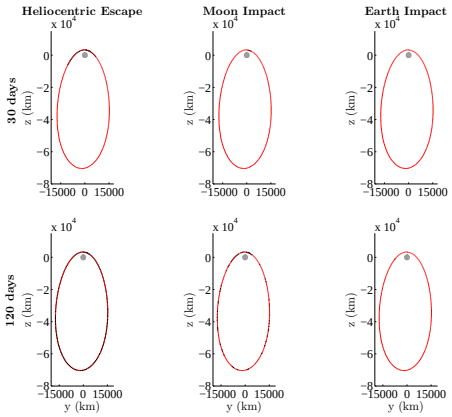

(b) 5 m/s Impulse Cases Within 30 and 120 day Time Frame.

Figure 15: Disposal Options from an $r_p = 4500$ km NRHO (L_2, South Family). The black dots indicate locations where the indicated disposal case (heliocentric escape, Moon impact, or Earth impact) is possible, given the correct impulse direction.

departure windows near periapsis exist for both heliocentric escapes and Moon impacts. The range of these windows is 4 hours and 0.4 hours respectively. Earth impact is not possible within 30 days. The 120 day results are largely similar to the 1 m/s impulse case: heliocentric escape is possible from any location, while Moon impacts are a combination of isolated locations and small windows of opportunity. Two notable differences exist. First, there is an increase in departure locations that lead to Moon impacts with the most obvious being a new window just before periapsis. Second, a single Earth-impacting disposal is found. Thus it is recommended to apply at least 5 m/s to target a specific disposal condition.

CONCLUSION

The Near Rectilinear Halo Orbit (NRHO) has been identified and studied for the purpose of using as a cislunar staging orbit. The NRHO may be initially defined to exist by its solution in the simplified CR3BP model, but a full ephemeris long term pseudo-stable orbit can be easily found quickly with the use of iterative numerical methods. Frequent access opportunities for Orion are feasible, selection of NRHO based on properties of eclipse avoidance mitigation are available, and multiple destinations ranging from various cislunar and heliocentric conditions are available for disposal of spent stages or for end of life operations. Thus, NRHOs are a viable candidate for long term cislunar operations and aggregation.

ACKNOWLEDGMENT

The authors wish to thank Jerry Condon and Roland Martinez for their support of this work, which was partially funded by NASA JSC under contract NNJ13HA01C.

NOTATION

CR3BP	Circular Restricted Three Body Problem
DRO	Distant Retrograde Orbit
EI	Entry Interface
LEO	Low Earth Orbit
LLO	Low Lunar Orbit
NRHO	Near Rectilinear Halo Orbit
NRI	NRHO Insertion
NRD	NRHO Departure
OME	Orion Main Engine
OPF	Outbound Powered Flyby
RPF	Return Powered Flyby
SLS	Space Launch System
TLI	Trans-Lunar Injection

REFERENCES

[1] K. Bocam, C. Walz, D. Bodkin, C. Pappageorge, V. Hutchinson, M. Dennis, and W. Cugno, "A Blueprint for Cislunar Exploration: A Cost-Effective Building Block Approach for Human Lunar Return," *AIAA Space 2012*, Sept. 2012.

[2] W. Pratt, C. Buxton, S. Hall, J. Hopkins, and A. Scott, "Trajectory Design Considerations for Human Missions to Explore the Lunar Farside from the Earth-Moon Lagrange Point EM-L2," *AIAA Space 2013*, Sept. 2013.

[3] R. Whitley and R. Martinez, "Options for Staging Orbits in Cislunar Space," *IEEE Aerospace 2015*, Mar. 2015.

[4] J. Breakwell and J. Brown, "The 'Halo' Family of 3-Dimensional Periodic Orbits in the Earth-Moon Restricted 3-Body Problem," *Celestial Mechanics*, Vol. 20, Nov. 1979, pp. 389–404.

[5] K. C. Howell and J. V. Breakwell, "Almost Rectilinear Halo Orbits," *Celestial Mechanics*, Vol. 32, Jan. 1984, pp. 29–52.

[6] D. Grebow, D. Ozimek, K. Howell, and D. Folta, "Multibody Orbit Architectures for Lunar South Pole Coverage," *Journal of Spacecraft and Rockets*, Vol. 45, Mar. 2008.

[7] D. Grebow, D. Ozimek, and K. Howell, "Design of Optimal Low-Thrust Lunar Pole-Sitter Missions," *The Journal of of the Astronautical Sciences*, Vol. 58, Jan. 2011.

[8] W. M. Folkner, J. G. Williams, and D. H. Boggs, "The Planetary and Lunar Ephemeris DE 421," *Interplanetary Network Progress Report*, Vol. 178, Aug. 2009, pp. 1–34.

[9] J. S. Parker and R. L. Anderson, *Low-Energy Lunar Trajectory Design*. Wiley, 2014.

[10] P. E. Gill, W. Murray, and M. A. Saunders, "SNOPT: An SQP Algorithm for Large-Scale Constrained Optimization," *SIAM J. on Optimization*, Vol. 12, Apr. 2002, pp. 979–1006.

[11] J. Williams, J. S. Senent, and D. E. Lee, "Recent Improvements to the Copernicus Trajectory Design and Optimization System," *Advances in the Astronautical Sciences*, Vol. 143, Jan. 2012.

[12] F. G. Lemoine, S. Goossens, T. J. Sabaka, J. B. Nicholas, E. Mazarico, D. D. Rowlands, B. D. Loomis, D. S. Chinn, D. S. Caprette, G. A. Neumann, D. E. Smith, and M. T. Zuber, "High-degree gravity models from GRAIL primary mission data," *Journal of Geophysical Research (Planets)*, Vol. 118, Aug. 2013, pp. 1676–1698.

[13] L. F. Shampine and H. A. Watts, "DEPAC - Design of a User Oriented Package of ODE Solvers," Technical Report SAND-79-2374, Sandia National Labs, Sept. 1980.

[14] C. Ocampo and J. Munoz, "Variational Equations for a Generalized Spacecraft Trajectory Model," *Journal of Guidance, Control, and Dynamics*, Vol. 33, Sept./Oct. 2010.

[15] D. C. Davis, S. A. Bhatt, K. C. Howell, J. Jang, R. L. Whitley, F. D. Clark, D. Guzzetti, E. M. Zimovan, and G. H. Barton, "Orbit Maintenance and Navigation of Human Spacecraft at Cislunar Near Rectilinear Halo Orbits," *27th AAS/AIAA Space Flight Mechanics Meeting*, Feb. 2017.

[16] G. Wawrzyniak and K. Howell, "An Adaptive, Receding-Horizon Guidance Strategy for Solar Sail Trajectories," *AIAA/AAS Astrodynamics Specialist Conference*, Aug. 2012.

[17] R. B. Roncoli, "Lunar Constants and Models Document," Tech. Rep. JPL D-32296, Jet Propulsion Laboratory, September 2005.

[18] J. Williams and G. L. Condon, "Contingency Trajectory Planning for the Asteroid Redirect Crewed Mission," *SpaceOps 2014 Conference*, May 2014. AIAA 2014-1697.

[19] R. Martinez, G. Condon, and J. Williams, "Time and Energy, Exploring Trajectory Options Between Nodes in Earth-Moon Space," Tech. Rep. JSC-CN-26397, Johnson Space Center, May 2012.